Textile & Leather Review

ISSN 2623-6281 | www.tlr-journal.com | 10.31881/TLR

3D Anthropometric Methods and Pattern Optimization for Ski Suit Design

Xiaotong Tang

How to cite: Tang X. 3D Anthropometric Methods and Pattern Optimization for Ski Suit Design. Textile & Leather Review. 2026; 9:6210-6228. https://doi.org/10.31881/TLR.2026.6210

How to link: https://doi.org/10.31881/TLR.2026.6210

Published: 24 November 2026

This work is licensed under a Creative Commons Attribution-ShareAlike 4.0 International License

3D Anthropometric Methods and Pattern Optimization for Ski Suit Design

Xiaotong Tang

Department of Fashion and Apparel Design, School of Fine Arts and Art Design, Qiqihar University, Qiqihar 161000, Heilongjiang, China
18645723198@163.com

Article
https://doi.org/10.31881/TLR.2026.6210
Published 24 November 2026

ABSTRACT

To address the issue of ski suit patterns failing to accurately adapt to movement postures due to a lack of dynamic anthropometric data, this paper introduces a pattern optimization method based on dynamic 3D measurement and parametric modeling that incorporates textile mechanical properties and fiber elasticity constraints. This approach synchronizes fabric deformation characteristics with body surface deformation and joint kinematics to ensure high-performance textile structures maintain ergonomic precision during complex high-speed maneuvers. First, a point cloud sequence of the wearer in typical skiing postures is captured using a multi-view synchronous scanning system. An improved ICP (Iterative Closest Point) algorithm based on FPFH is then used for high-precision spatiotemporal registration to construct a dynamic human digital model. Next, an SMPL (Skinned Multi-Person Linear) model embedded in the motion deformation domain is driven for parametric fitting, decoupling joint displacement and surface deformation parameters. Finally, these parameters are input into a pre-trained GNN pattern generator. This network uses the front and back bodice patterns as graph inputs and directly outputs the optimized garment outline and dart structure through graph convolution and pooling operations. Experimental results show that the optimized pattern improves the gap value in the knee region by 71.2% compared to the traditional pattern. This method establishes a closed-loop technical path for the digital design of functional sportswear by integrating dynamic human biometrics with textile material behavior. By synchronizing fiber mechanical response with high-speed movement data, the system ensures that textile structures are precisely engineered for optimal ergonomic performance.

KEYWORDS

3D anthropometry, pattern optimization, ski suit design, SMPL model, textile structures

INTRODUCTION

Three-dimensional anthropometry serves as a digital bridge connecting human morphology with textile structural engineering, providing the essential data support required for the precise spatial arrangement of high-performance fibers. This integration allows for the alignment of fabric mechanical properties with physiological contours to optimize the ergonomic efficiency of specialized sports equipment. Ski suits, as typical professional protective equipment, require design to address multiple contradictions in extreme environments, including wind and water resistance, movement flexibility, and thermal and moisture comfort [1,2]. This places demands on the matching accuracy between the pattern and dynamic human form far exceeding those of conventional clothing. Therefore, constructing a dedicated human database for skiing and driving pattern optimization has clear engineering value for improving the ergonomic performance and athletic performance of equipment.

Current research faces clear challenges in acquiring dynamic human data suitable for ski suit design. Skiing movements involve multi-joint complex movements such as forward trunk leaning, deep hip and knee flexion, and large upper limb swings [3,4], resulting in complex and asymmetrical deformation of the human soft tissue. This renders traditional three-dimensional scanning data based on standard standing posture meaningless. Although motion capture systems can record skeletal movement trajectories, they struggle to directly acquire precise three-dimensional geometric changes on the body surface while wearing basic clothing layers [5,6]. Furthermore, the ease distribution rules relied upon by existing clothing pattern design theories are mainly based on experience under static or limited movement conditions, lacking a quantitative model that describes the dynamic interaction between skin stretching and clothing space during intense, continuous movement [7,8]. This often results in undue restraint or redundancy in the designed patterns at key movement points. Some studies have attempted to improve the performance of skiwear by increasing ease in specific areas, such as increasing the range of motion in the knee joint area. However, this method lacks systematicity and is difficult to adapt to the complex changes in different body types and movement postures.

For dynamic anthropometric measurements, non-contact optical scanning is the mainstream technology, and existing research has employed multi-camera systems to capture periodic movements. However, there are still technological gaps in the rapid scanning and high-precision point cloud stitching for non-periodic, low-stability postures such as skiing. Existing algorithms lack stability in identifying feature points on large areas of uniformly colored tight-fitting fabric [9,10]. Regarding pattern generation, parametric human models such

as SMPL provide a framework for analyzing body shape variability, but their standard models lack the ability to model extreme postures caused by professional sports [11,12]. Some studies have attempted to import motion capture data into virtual fitting software for pattern evaluation; however, this method relies on the "black box" physics engine of commercial software, and its simulation results are difficult to reverse-engineer for structural parametric adjustments of the pattern [13,14]. Therefore, establishing an end-to-end method from skiing posture-specific 3D measurement to data-driven pattern optimization remains an unresolved issue. The key lies in the lack of an intelligent design chain that can directly and automatically map dynamic body surface deformation parameters to clothing structural parameters.

To address the aforementioned challenges, this paper introduces a pattern optimization method based on dynamic 3D anthropometric measurement and parametric modeling, directly connecting dynamic human body data with garment structural design. First, a multi-view synchronous scanning platform is constructed, and a scanning protocol covering typical skiing turns and downhill postures is designed. A sequential point cloud registration method integrating color-coded features and the ICP algorithm is employed to reconstruct a high-fidelity dynamic human body model. Next, an extended SMPL model embedding skiing motion deformation priors is developed to decouple the scanned data into a vertex displacement field dependent on body shape parameters and posture: the set of displacement vectors of vertices on the human body surface relative to the base model. Finally, a GCN (Graph Convolutional Network) is trained, representing the base pattern with a graph structure and using the vertex displacement field as conditional input. As an implementation of GNN, this network learns to directly map dynamic surface deformation to changes in garment structural parameters, outputting an optimized 2D garment contour. This research establishes a repeatable dynamic anthropometric solution for skiing and forms a data-driven closed loop for functional pattern optimization that accounts for textile elongation and fiber tensile performance. This integration promotes a paradigm shift in sportswear design from static experience to dynamic precision by synchronizing fabric mechanical responses with the deformation requirements of the human body during motion.

Overall Technical Approach

This study establishes a comprehensive technical roadmap from dynamic anthropometry to skiwear pattern optimization. Multi-view synchronous scanning acquires ski-posture point cloud sequences, and further improved algorithms achieve high-precision dynamic human reconstruction. The SMPL model is further extended to decouple dynamic deformation features, and GNN pattern generator maps deformation parame-

ters to garment structure parameters. The above technical roadmap includes three technical components: dynamic measurement, parameter decoupling and intelligent pattern generation. The closed-loop design process is achieved from human motion data to functional clothing structure.

Figure 1 process flow from data collection to pattern optimization showing the data flow and processing logic for each data flow between processes. Highlighting the three processes of dynamic anthropometrics, parameter decoupling, and pattern generation, as well as their nodes, intuitively demonstrating the compre -hensiveness and systematicity of the research process.

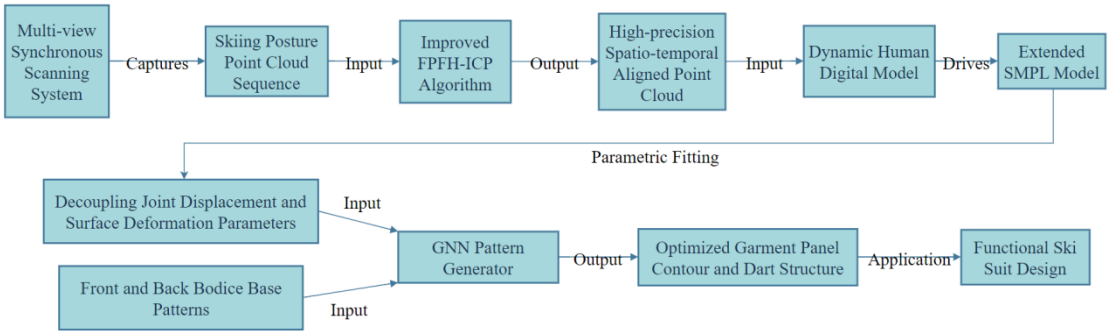


Figure 1. Overall technical route

Dynamic 3D Data Acquisition and Reconstruction for Skiing Postures

The multi-view optical scanning system includes eight structured light 3D scanners [15,16]. These eight scanners are arranged in a ring around a 2.5 m circular area with an angle of 45 degrees between any two adjacent ones. The height of the scanners is fixed at 1.5 m so that the entire human body from head to ankle can be captured. These scanners work in global shutter mode and are synchronized in time with sub-millisecond accuracy by the hardware synchronization controller to make the data collected from these eight views temporally consistent. In addition, the multi-view optical scanning system uses a high-power LED light source with wavelength of 850 nm, which can avoid interference from ambient light and improve the accuracy of the collected 3D model [17,18]. These eight scanners are connected to the central control unit through gigabit Ethernet to achieve real-time transmission and centralized processing of data [19,20].

A total of thirty two subjects participated in the dynamic scanning experiment, comprising sixteen males and sixteen females. Their body dimensions spanned a representative range of the skiing population, with statures from one point five seven meters to one point eight nine meters. This distribution ensured that the captured point cloud sequences incorporated sufficient morphological variability to inform the extension of the SMPL

model. The material of the bodysuit was dark gray spandex, which is stretchable and has low reflectance. Circular fluorescent markers with diameter of 3 mm were attached to 12 typical anatomical parts of the body, including acromion, lateral part of elbow, wrist, anterior superior iliac spine, lateral knee and lateral ankle. The seven typical postures of skiing included basic downhill posture, giant slalom transition posture, small slalom transition posture, turn completion posture, ready posture, standing relaxed posture and jump landing posture. Each posture was maintained for three seconds with a scanning frequency of thirty frames per second to acquire high-fidelity static surface geometry at key instants of skiing motion. This set of discrete postures encompasses the extreme body configurations encountered during skiing and provides the geometric basis for subsequent parametric modeling and pattern optimization. The scanning environment temperature was controlled at 22±1℃, and the humidity was maintained at 50±5% to maintain consistent material properties of the spandex suit, as variations in these conditions can alter fabric tension and skin friction, thereby affecting the geometric fidelity of the captured point cloud data.

Point cloud registration employed an improved ICP algorithm, which integrates color coding features, artificial marker constraints, and FPFH features [21,22]. The attachment points of the fluorescent markers were reinforced with high-adhesion medical-grade double-sided tape to maintain positional stability during high-impact movements. Prior to each scanning session, the fit of the spandex suit was adjusted to minimize relative displacement between the fabric and the skin. During post-processing, markers exhibiting trajectory inconsistencies across consecutive frames were identified through optical flow analysis and excluded from the registration constraint set. This procedure ensures that the anatomical landmarks used in the improved ICP objective function remain representative of the underlying skeletal references throughout the dynamic sequence. To address the limited color information caused by the single color of the ski bodysuit, the system obtained pseudo-color information through phase coding of multi-view light sources. For point cloud P_k in frame k and point cloud P_{k+1} in frame k +1, define a feature matching function:

$$F(P_k, P_{k+1}) = \sum_{i=1}^{N} \omega_i \parallel f(p_i) - f(q_i) \parallel^2 \quad (1)$$

Let $p_i \in P_k$, $q_i \in P_{k+1}$, $f(p_i)$ represent the FPFH feature descriptor for point p_i , N be the number of matching point pairs, and ω_i be the adaptive weight coefficient. The FPFH feature descriptor is calculated as follows:

$$FPFH(p_i) = [d_1, d_2, ..., d_{33}]^T \tag{2}$$

d_j is the j -th feature component, obtained by calculating the geometric relationship between point p_i and its k nearest neighbors, including the distance, angle and curvature information between points. The 33-dimensional structure of the feature vector contains a combination of 11 simplified point feature histograms. To address the sparse surface features of ski suits, an artificially marked point constraint term is introduced [23]. The improved ICP objective function is expressed as:

$$E(R,t) = \sum_{i=1}^{M} \| Rp_i + t - q_i \|^2 + \lambda \sum_{j=1}^{L} \| Rm_j + t - n_j \|^2 \tag{3}$$

R is the rotation matrix; t is the translation vector; M is the number of automatically matched point pairs; L is the number of manually labeled point pairs; m_j is the coordinate of the labeled point in the previous frame; n_j is the coordinate of the labeled point in the next frame; and λ is the label constraint weight coefficient, with a value range of [0.5, 1.5], which is dynamically adjusted according to the visibility of the labeled points. By minimizing this objective function, accurate spatial transformation parameters between frames are obtained, achieving high-precision spatiotemporal registration of the point cloud sequence [24,25]. The registered point cloud sequence generates a continuous dynamic human body surface model through a triangular mesh reconstruction algorithm, providing a geometric basis for subsequent parametric modeling [26,27].

Figure 2 illustrates the complete process of dynamic point cloud registration, including input point cloud sequence, data preprocessing, dual-path feature extraction, objective function construction, spatial transformation parameter calculation, and triangular mesh reconstruction.

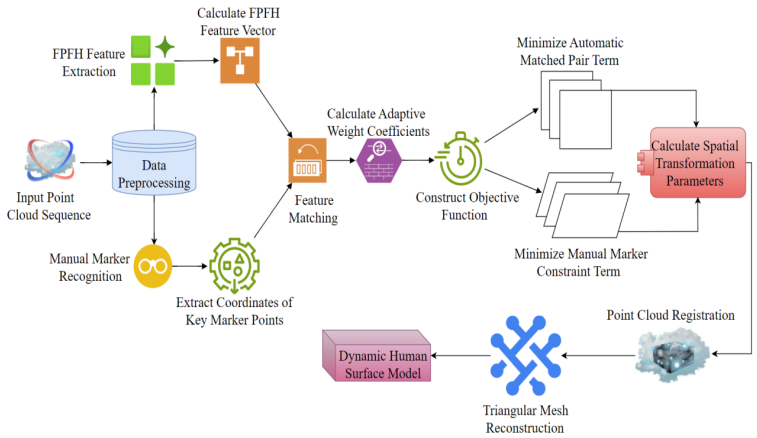


Figure 2. Dynamic point cloud registration algorithm for skiing posture

Dynamic Human Parametric Modeling Based on Extended SMPL Model

The SMPL model, as the basic framework for parametric human modeling, generates human meshes through a linear combination of body shape and posture parameters [28,29]. Traditional models have limitations in representing extreme skiing postures, making it difficult to accurately describe special postures such as deep knee flexion and forward trunk lean during skiing [30,31]. To address this issue, an extended SMPL model is constructed. This model adds a quadratic constraint dimension of the knee flexion-extension rotation axis to the original 23 joint rotational degrees of freedom, and introduces a nonlinear hybrid shape compensation term for hip internal and external rotation.

The equation for calculating the vertex position of the extended SMPL model is:

$$V(\beta,\theta) = W(T(\beta) + \sum_{i=1}^{K} \theta_i B_i, J(\beta), \theta) \tag{4}$$

$V \in R^{N\times 3}$ represents the 3D coordinates of N vertices; $\beta \in R$ is the body shape parameter; $\theta \in R^{72}$ the pose parameter; W is the skinning weight function; $T(\beta)$ is the basic body shape template; B_i is the pose blending shape; and $J(\beta)$ is the joint position calculated based on the body shape parameters. The extension part enhances the model's ability to represent skiing postures by modifying the blending shape coefficients β_{10} is related to the knee and hip joints in B_i .

For the characteristics of skiing, the joint rotation constraint function is defined as follows:

$$C(\theta) = \sum_{j\in K} w_j(\theta_j - f(\theta_k))^2 \tag{5}$$

K represents the set of joints requiring special constraints, including the knee and hip joints; θ_j is the rotation angle of the j-th joint; θ_k is the rotation angle of the associated joint; $f(\cdot)$ is a nonlinear mapping function established based on skiing kinematics analysis; and w_j is the joint weight coefficient, determined according to sports biomechanics research. This constraint function is embedded into the optimization objective of the SMPL model to ensure that the generated human posture conforms to the physiological laws of skiing.

The dynamic point cloud sequence is fitted with the extended SMPL model to construct a nonlinear optimization problem:

$$\min_{\beta,\theta,D} \| P - V(\beta,\theta) - D \|_F^2 + \lambda_1 \| \beta \|_2^2 + \lambda_2 \| \theta - \theta_0 \|_2^2 + \lambda_3 \| C(\theta) \|_2^2 \quad (6)$$

$P \in R^{N\times 3}$ represents dynamic point cloud data; $D \in R^{N\times 3}$ represents the vertex displacement field; θ_0 represents the initial posture parameters, and λ_1 , λ_2 , and λ_3 represent regularization coefficients, controlling the smoothness of body shape parameters, the amplitude of posture changes, and the strength of joint constraints, respectively. The optimization problem is solved using the L-BFGS (Limited-memory Broyden–Fletcher–Goldfarb–Shanno) algorithm [32,33]. Body shape parameters, posture parameters, and vertex displacement fields matching the skiing posture are obtained. The vertex displacement field D characterizes the local deformation of the skin surface relative to the basic SMPL model during skiing, providing key input for subsequent pattern optimization.

Adaptive Optimization of Pattern Parameters Based on GCN

The basic pattern of the ski suit is structured into a graph representation. The front, back, and sleeves are each constructed as independent graph structures. Key points of the garment outline are defined as graph nodes, and the garment structure lines and dart lines constitute graph edges. The graph structure is represented as $G = (V, E)$, where V is the set of nodes and E is the set of edges. The node feature vector $v_i \in R^d$ contains the two-dimensional coordinates and curvature information of the node, where d represents the feature dimension. The edge feature $e_{ij} \in R^m$ describes the geometric relationship between nodes, where m is the edge feature dimension. The basic pattern graph structure obtains an initial set of node coordinates $P_0 = \{p_0^1, p_0^2, ..., p_0^n\}$ through preprocessing, where $p_0^i = (x_0^i, y_0^i)$ represents the two-dimensional coordinates of the i -th node, and n is the total number of nodes.

The GCN receives a dynamic human vertex displacement field as a conditional input, which is obtained by decoupling through an extended SMPL model. The network contains four graph convolutional layers and two graph pooling layers. The graph convolution operation in each layer is defined as [34,35]:

$$h_i^{(l+1)} = \sigma\left(\sum_{j\in N(i)} \frac{1}{\sqrt{|\ N(i)\ |\ |\ N(j)\ |}} W^{(l)} h_j^{(l)} + b^{(l)} \right) \quad (7)$$

Let $h_i^{(l)}$ represent the feature vector of the i -th node in the l-th layer, $N(i)$ be the neighborhood set of node i , $W^{(l)} \in R^{d_{l+1} \times d_l}$ be the learnable weight matrix, $b^{(l)} \in R^{d_{l+1}}$ be the bias term, σ be the nonlinear activation function, and d_l represent the feature dimension of the l -th layer. The graph pooling operation employs a max pooling strategy, retaining the node with the largest feature response and its neighborhood structure.

The conditional generation process is implemented through a feature fusion layer, fusing the human vertex displacement field $\Delta \in R^{k \times 3}$ with the basic pattern graph features, where k represents the number of vertices in the human model. The fusion layer outputs the node coordinate offset $\Delta P = \{\delta p^1, \delta p^2, ..., \delta p^n\}$, where $\delta p^i = (\delta x^i, \delta y^i)$ is the two-dimensional coordinate offset of the i -th node. The optimized clothing piece contour coordinate set is represented as:

$$P_{opt} = P_0 + \Delta P \tag{8}$$

The final output includes the 2D garment outline and dart structure parameters, completing the mapping transformation from dynamic human body deformation to a functional pattern. The network training employs a mean squared error loss function to minimize the geometric difference between the network's output coordinates and the target coordinates.

EXPERIMENTAL DESIGN AND RESULT ANALYSIS

Experimental Data and Evaluation Setup

In order to prepare the experimental data and evaluation setup, the multi-source data fusion method was used to build the training dataset. The basic 3D human scan data was extracted from the public CAESAR (Civilian American and European Surface Anthropometry Resource) anthropometric database, which contains 200 3D human scans in specified standing position. The basic 3D human shape variability model was built based on the 3D human scans. Different gender and age were included in the basic training dataset. And the complete anthropomorphic measurement data and point cloud data were included as well, which provided the basis for the body shape distribution in the subsequent parametric model. SMPL produced the simulated dynamic human body sequences through principal component analysis of the CAESAR database. This subset comprises 40 representative body shapes capturing dominant morphological variance combined with 7 typical skiing postures for method training and validation. Feature space expansion via data augmentation secured

GNN convergence and generalization across diverse morphologies. The basic ski suit pattern adopted industry standard paper patterns, including three common sizes: M, L, and XL, serving as the initial input conditions for the pattern optimization algorithm. As shown in Table 1.

Table 1. Key Statistical Information of Experimental Dataset

Data type	Source	Sample size	Posture category	Main purpose
Basic 3D human body scan data	CAESAR database	200 cases	Standard stance	Build base body shape variability
Simulate dynamic human body sequence	SMPL model generation	40 body types x 7 skiing postures	Basic Descent,Large Turn Transition, Small Turn Transition,Turn End,Preparation, Standing Relaxation, Jump Landing	Method training and validation
Basic ski suit fit	Industry standard pattern	3 sizes (M, L, XL)	-	Optimization algorithm initial input

The experimental design employed a control group validation strategy. Group A generated ski suit patterns based on dynamic data and GNN optimization, while Group B generated patterns based on the same basic body type but using static posture and traditional proportional allocation methods. Performance was compared between the two groups in a virtual try-on session. The virtual try-on session used precise fabric mechanical parameters, including warp and weft tensile modulus, shear modulus, and flexural stiffness. A nonlinear spring-damping system was used to simulate the interaction between the human body and clothing in the contact model.

Accuracy Analysis of Dynamic Human Body Reconstruction and Parametric Decoupling

Considering the characteristics of human posture in skiing, this paper investigates accuracy performance of dynamic human body reconstruction and parametric decoupling process by analyzing geometric error distribution characteristics of skiing gait six typical anatomical regions based on seven typical skiing postures. Because of the forward leaning posture, the shoulders and hips are the main transitional area of the torso; The elbows and wrists represent the soft tissue deformation of upper limbs during the swing; The knees and ankles are directly related to the joint flexion and ground reaction force in the process of skiing. The error data of above four areas are used for pattern designing of ski suit. Registration error represents the geometric error between the original point cloud and registration model, which reflects the accuracy of dynamic scanning and registration algorithm; Fitting error represents the fitting degree of parametric model to the registered point

cloud, which reflects the applicability of extended SMPL model under different skiing postures. As shown in Fig.3, the error distribution and standard deviation of each region under different postures are analyzed. Figure 3 (a) registration error reaches the peak in jump landing posture, with the knee error of 3.78 mm and 34.0% more than that in standing relaxed posture. This is because the soft tissue deformation is extremely severe in jump landing skiing posture due to the high impact force on the knee joint. Elbow error also increases from 2.87 mm in the posture transition from small turn to 3.02 mm in the jump landing posture, which represents the continuous swinging effect of the upper limb in the landing process of high-speed turn. Figure 3 (b) Fitting error is generally higher than registration error, and the knee error reaches 5.87 mm in jump landing posture, which means it is difficult to fit the parametric model into the highly dynamic posture with complicated deformation. The error of ankle area is still in a low level, and only 2.05 mm in basic downhill posture, because the mechanical property in this area is relatively stable during the skiing movement. Error distribution pattern verifies the correctness of the dynamic measurement and parametric decoupling method in different skiing postures, and establishes an accurate geometric basis for the following virtual fitting and pattern optimization.

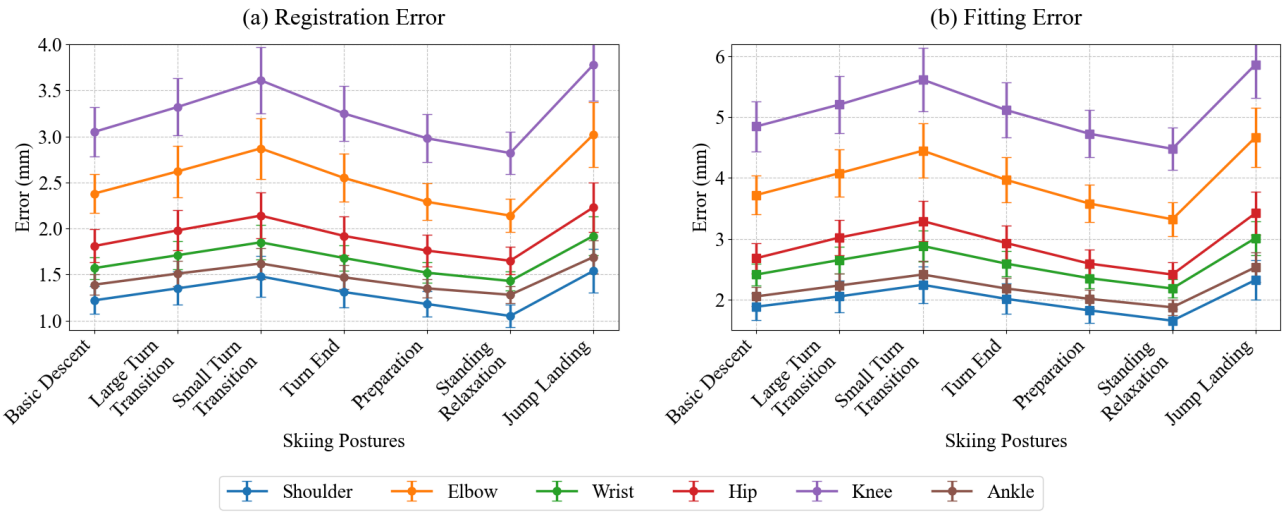


Figure 3. Comparison of registration and fitting error distributions in key regions under different skiing postures: (a) Registration Error; (b) Fitting Error

Knee joint requires eight to twelve millimeters of movement space during deep flexion postures, exceeding the 5.87 millimeter fitting error magnitude. Fabric elastic deformation capacity compensates for geometric deviations at this scale. Garment structural design allocates ease allowances at centimeter level adjustments,

rendering millimeter-scale model fitting errors acceptable. Dynamic anthropometry aims to capture deformation trends in critical regions.

Comparative Analysis of Virtual Wearing Performance Before and After Pattern Optimization

In order to verify the practical effect of the pattern optimization technology based on dynamic anthropometry in the design of skiwear, virtual try-on performance comparison experimental system is established. Group A pattern based on dynamic 3D anthropometry and GNN optimization method were comprehensively compared with group B pattern based on static postures and traditional proportioning method. Gap layer layer distribution, as the spatial distance distribution characteristics between human body and clothing, is an important index to reflect clothing motion performance. It directly reflects the spatial relationship between the human body and clothing, and its magnitude and distribution shape affect the degree of freedom of movement and thermal and moisture comfort. Especially in key postures such as deep knee flexion during skiing, a reasonable gap distribution plays a decisive role in avoiding movement restriction and improving equipment efficiency. The experiment selected a typical downhill posture as the test scenario. Human-clothing gap data for both groups of patterns were obtained through a high-precision virtual try-on system. Figure 4 shows the comparison results of the gap layer distribution of the two groups of patterns under a unified coordinate system.

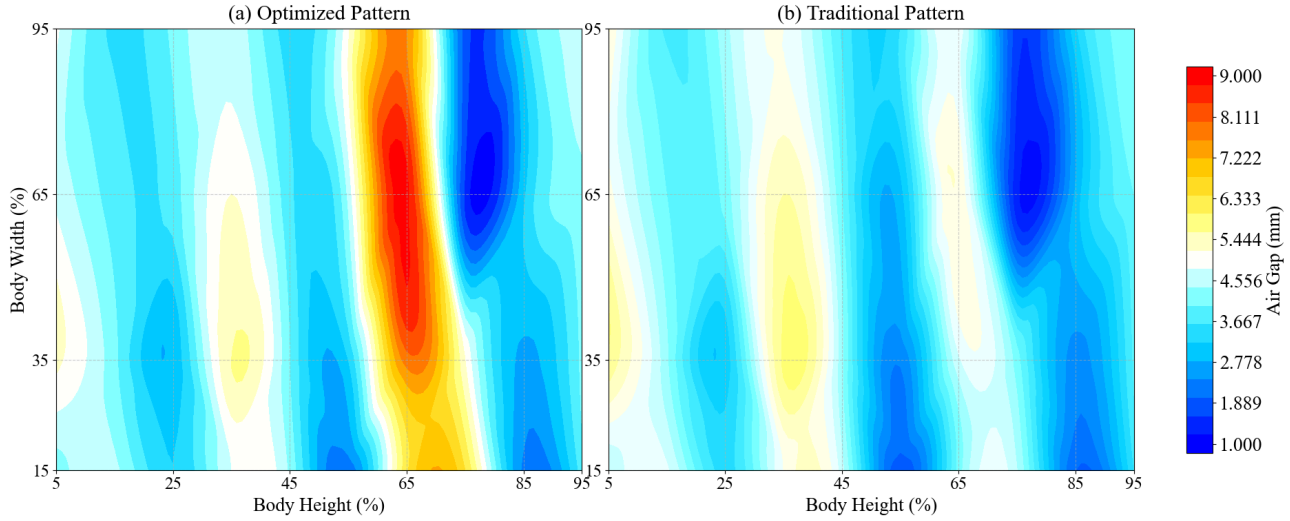


Figure 4. Comparison of body-clothing gap layer distribution between optimized and traditional ski suit patterns in a downhill posture: (a) Optimized Pattern; (b) Traditional Pattern

Figure 4(a) shows that the optimized design creates a significant concentration of gaps in the knee area (65% height), with a maximum value of 8.9 mm, far exceeding the distribution levels in the shoulder and ankle areas. This distribution pattern closely matches the soft tissue deformation caused by the high impact force on the knee joint during skiing. In Figure 4(b), the maximum gap value in the knee area of the traditional design is only 5.2 mm, and the distribution is more uniform, failing to reflect targeted design for key movement areas. The optimized design increases the gap value in the knee area by 71.2% compared to the traditional design. The difference is that the dynamic measurement method reflects the surface deformation features of the knee joint in the deep flexion posture of the skiing standing and the traditional way only according to the standing postural data of static data can cause insufficient mobility in the relevant parts, the difference in gap distribution will directly affect the function of the ski suit in actual exercise. By increasing the knee mobility space rationally, the optimization design reduces the restrictive effect on the strenuous exercise in the traditional design and gives the skiers a biomechanically appropriate movement space. The gap distribution characteristics of the optimized pattern in the key movement area show the important supporting effect of the dynamic anthropometric data in the functional clothing.

Correlation Analysis of Pattern Parameter Variation and Human Body Deformation

Considering the mapping relationship between dynamic human body deformation and ski suit pattern parameters is complicated, this study analyzes vertex displacement field unconnected with extended SMPL model. It takes seven typical skiing postures as objects and quantitatively studies the correlation between skin stretch characteristic in gait joint area and the relative change of pattern parameter. The basic downhill is the stable state of skiing; the turn-ending posture is the instantaneous characteristic of posture change under the condition of turning from giant to small turns; the ready and relaxed standing posture is the typical low-dynamic posture; the jump landing is the extreme condition with high impact. The skin stretch rate is the quantitative description of surface deformation; it can directly reflect the degree of stretching of soft tissue during the movement. The rear knee dart spread and armhole depth adjustment are two structural parameters that affect the performance of ski suit; the former is used to limit the degree of freedom of movement of the knee joint; the latter is used to limit the range of upper limb swing. Figure 5 shows the relationship between skin stretch rate and corresponding pattern parameter changes in the knee and elbow joint areas.

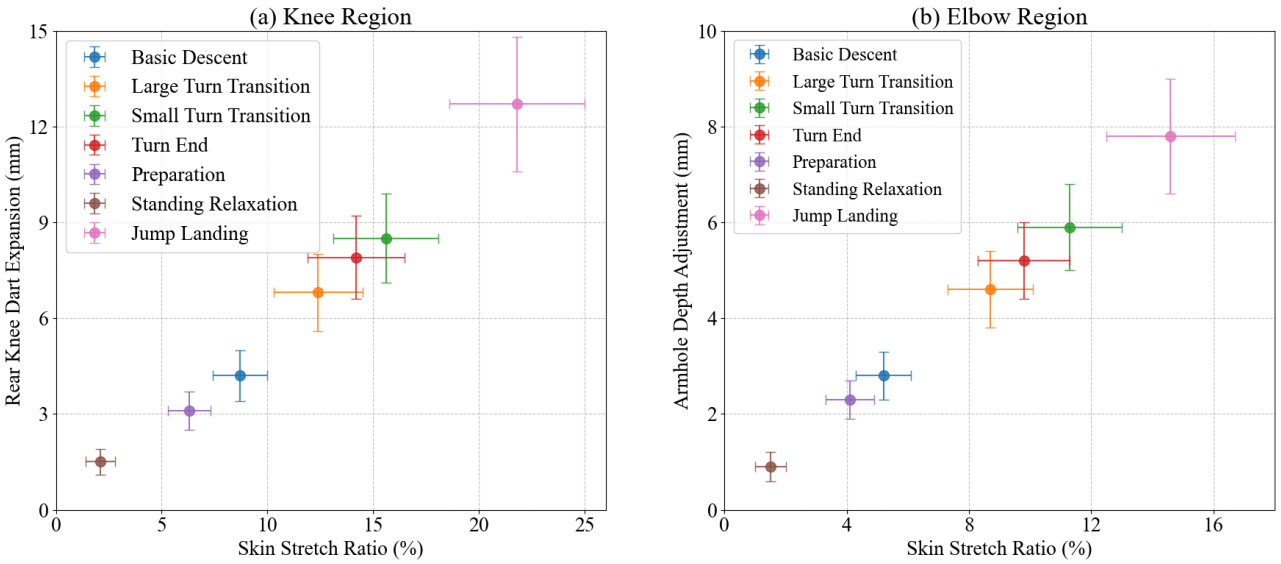


Figure 5. Correlation analysis between skin stretching rate and posterior knee septum expansion in the knee region: (a) Knee Region; (b) Elbow Region

Figure 5(a) shows that the skin stretch rate of the knee joint area reaches 21.8% in the jump landing posture, corresponding to a rear knee septum extension of 12.7 mm, which is the highest value among all postures, indicating that the knee area requires maximum range of motion under extreme impact postures. In the standing relaxed posture, the skin stretch rate is only 2.1%, and the rear knee septum extension is 1.5 mm, reflecting the minimum range of motion requirement in the static posture. Figure 5(b) shows that the skin stretch rate of the elbow joint area in the jump landing posture is 14.6%, and the armhole depth adjustment is 7.8 mm, which is also at the maximum value, while the corresponding parameters in the standing relaxed posture are 1.5% and 0.9 mm. The skin stretch rate of the knee joint area is generally higher than that of the elbow joint area, which is consistent with the biomechanical characteristics of the knee joint bearing greater impact force in skiing. The changes in the pattern parameters of both joint areas increase with the increase of skin stretch rate, verifying that the pattern optimization method based on dynamic anthropometrics can accurately capture the deformation requirements of key parts of the movement. This correlation analysis confirms that the data-driven pattern optimization method has clear biomechanical basis and engineering applicability.

CONCLUSION

This paper constructs a dynamic anthropometric and pattern optimization system for skiing by mapping human motion deformation data directly to functional patterns while incorporating textile mechanical

anisotropy and fiber strain variables. By synchronizing these kinetic measurements with the elongation properties of high-performance fabrics, the system ensures that textile structural layouts precisely accommodate the complex geometric changes of the body during high-speed maneuvers. A multi-view synchronous scanning system is proposed to accurately acquire the surface geometric variation information of skiing postures. An improved ICP algorithm is designed to solve the difficult problem of feature points extraction in fitting clothes fabrics tightly. Furthermore, an extended SMPL model improves the extreme posture representation ability by adding skiing kinematic constraints. The GNN pattern generator establishes the quantitative relationship between skin stretch rate and structural parameters. Compared with traditional methods, the gap performance in the knee region improves 71.2%. The experimental data show that the dynamic measurement based pattern optimization can accurately respond to the deformation requirements of the deformation area, which solves the problem of unsystematic allocation of activity margin in traditional design. This method replaces static measurement and experience-driven design with a repeatable technical route for digital R&D that integrates textile mechanical behavior and fiber elasticity into high-performance sportswear development. By transitioning from subjective intuition to dynamic precision, the framework provides essential technological support for the intelligent design of functional textile structures optimized for athletic movement.

Author Contributions

Xiaotong Tang designed, collected and analyzed the data, and drafted the manuscript. Xiaotong Tang conducted the study, critically revised the manuscript for important intellectual content, and gave final approval of the version to be published. Xiaotong Tang participated fully in the work, take public responsibility for appropriate portions of the content, and agreed to be accountable for all aspects of the work in ensuring that questions related to the accuracy or integrity of any part of the work are appropriately investigated and resolved.

Conflicts of Interest

The author declareS no conflict of interest.

Funding

This research was supported by,

1.The Basic Research Business Special Project of the Education Department of Heilongjiang Province in 2023, titled “Research on Innovative Design of Functional and Fashionable Tourism Skiwear” (Project No. 145209230)

2.General Project of Art Science Planning in Heilongjiang Province, 2024 Project “Research on the Development Strategy of Cross border Ethnic Costume Art between China and Russia” Project Number: 2024C017

3.Basic Research Business Special Project of Heilongjiang Provincial Department of Education in 2024, Project No. 145409504: Research on Innovative Transformation of Ice and Snow Art

Acknowledgements

Not applicable.

REFERENCES

[1] Ren L, Yang C, Zhou Z. Cross-Cultural Innovative Ski Wear Design from the Perspective of Cultural Symbol Translation. Textile and Leather Review. 2024; 7(1):1346-1359. doi: 10.31881/TLR.2024.161

[2] Zhang B, Ramirez-Gomez A, Wang J, et al. Bionic design of knitted fabrics for ice and snow sports. Textile Research Journal. 2024; 94(13-14):1470-1483. doi: 10.1177/00405175241228526

[3] Brandt T, Ebel C, Lebahn C, et al. Acute physiological responses and performance determinants in Hyrox©-a new running-focused high intensity functional fitness trend. Frontiers in Physiology. 2025; 16(1): 1519240-1519252. doi: 10.3389/fphys.2025.1519240

[4] Koon L M, Donnelly J E, Sherman J R, et al. Feasibility and Preliminary Effects of Community-Based High-Intensity Functional Training for Adults with Mobility Disabilities and Overweight/Obesity: A Pilot Study. Sports. 2025; 13(10): 361-380. doi: 10.3390/sports13100361

[5] Moniruzzaman M, Yin Z, Hossain M S B, et al. Wearable motion capture: Reconstructing and predicting 3d human poses from wearable sensors. IEEE Journal of Biomedical and Health Informatics. 2023; 27(11):5345-5356. doi: 10.1109/JBHI.2023.3311448

[6] Niu Z, Lu K, Xue J, et al. From methods to applications: A review of deep 3D human motion capture. IEEE Transactions on Circuits and Systems for Video Technology. 2024; 34(11):11340-11359. doi: 10.1109/TCSVT.2024.3423411

[7] Zhang Y, Liu C. Unlocking the potential of artificial intelligence in fashion design and e-commerce applications: The case of Midjourney. Journal of Theoretical and Applied Electronic Commerce Research. 2024; 19(1):654-670. doi: 10.3390/jtaer19010035

[8] Huang X, Kettley S, Lycouris S, et al. Autobiographical design for emotional durability through digital transformable fashion and textiles. Sustainability. 2023; 15(5):4451-4472. doi: 10.3390/su15054451

[9] Seckin M, Seckin A C, Demircioglu P, et al. FabricNET: a microscopic image dataset of woven fabrics for predicting texture and weaving parameters through machine learning. Sustainability. 2023; 15(21):15197-15214. doi: 10.3390/su152115197

[10] Meeradevi T, Sasikala S, Gomathi S, et al. An analytical survey of textile fabric defect and shade variation detection system using image processing. Multimedia Tools and Applications. 2023; 82(4):6167-6196. doi: 10.1007/s11042-022-13575-8

[11] Feng W, Li X, Wang J, et al. Status of research on parametric methods for the reconstruction of 3D models of the human body for virtual fitting. International Journal of Clothing Science and Technology. 2024; 36(2):338-356. doi: 10.1108/IJCST-06-2023-0086

[12] Bataineh A M, Mohamed A S A. Monocular 3D Human Pose Estimation for REBA Ergonomics: A Critical Review of Recent Advances. Computers, Materials & Continua. 2025; 84(1):93-124. doi: 10.32604/cmc.2025.064250

[13] Ciorna V, Melancon G, Petry F, et al. Interact: A visual what-if analysis tool for virtual product design. Information Visualization. 2024; 23(2):123-141. doi: 10.1177/14738716231216030

[14] Cai C H. MP: motion program synthesis with machine learning interpretability and knowledge graph analogy. Automated Software Engineering. 2025; 32(1):21-60. doi: 10.1007/s10515-025-00495-8

[15] Wan M, Zheng R, Wang S, et al. Efficient 3D scanning measurement system based on asymmetric trinocular vision and a multi-line laser. Applied Optics. 2023; 62(8):2145-2153. doi: 10.1364/AO.481406

[16] Pyle D N, Candusso D. Multi-camera photogrammetry for 3D scanning cultural garments. Digital Applications in Archaeology and Cultural Heritage. 2025; 37(1):e00430-e00442. doi: 10.1016/j.daach.2025.e00430

[17] Wu H, Guo R, Wan J, et al. Underwater polarimetric imaging system for real-time de-backscatter video application. Optics & Laser Technology. 2026; 197(1):114654-114664. doi: 10.2139/ssrn.5604787

[18] Luo L, Shan S, Li X. A review: Laser interference lithography for diffraction gratings and their applications in encoders and spectrometers. Sensors. 2024; 24(20):6617-6660. doi: 10.3390/s24206617

[19] Goyal R, Elawadhi O, Sharma A, et al. Cloud-connected central unit for traffic control: interfacing sensing units and centralized control for efficient traffic management. International Journal of Information Technology. 2024; 16(2): 841-851. doi: 10.1007/s41870-023-01527-w

[20] Passaretti D, Steiger M, Pionteck T. Enabling plug-and-play in cyber-physical systems using MPSoC-FPGAs. IEEE Access. 2023; 11(1):116219-116234. doi: 10.1109/ACCESS.2023.3325742

[21] Sun R, Zhang E, Mu D, et al. Optimization of the 3D point cloud registration algorithm based on FPFH features. Applied sciences. 2023; 13(5):3096-3109. doi: 10.3390/app13053096

[22] Lian Z, Wang X, Lin J, et al. Second-order Spatial Measures Low Overlap Rate Point Cloud Registration Algorithm Based On FPFH Features. AI Communications. 2024; 37(4):599-617. doi: 10.3233/AIC-230217

[23] Qi J, Li D, He J, et al. Optically non-contact cross-country skiing action recognition based on key-point collaborative estimation and motion feature extraction. Sensors. 2023; 23(7):3639-3662. doi: 10.3390/s23073639

[24] Shen S, Ito T, Hirose T. Spatio-Temporal Gradient Flow for Efficient Motion Estimation in Sparse Point Clouds. Journal of Robotics and Mechatronics. 2025; 37(6):1327-1342. doi: 10.20965/jrm.2025.p1327

[25] Wu S, Ren L, Zhu E. Fast Motion State Estimation Based on Point Cloud by Combing Deep Learning and Spatio-Temporal Constraints. Applied Sciences. 2024; 14(19):8969-8985. doi: 10.3390/app14198969

[26] Chen D, Song Y, Liang F, et al. 3D human body reconstruction based on SMPL model. The Visual Computer. 2023; 39(5):1893-1906. doi: 10.1007/s00371-022-02453-x

[27] Yang Y, Zhang H, Fernández A B, et al. Digitalization of 3-D human bodies: A Survey. IEEE Transactions on Consumer Electronics. 2024; 70(1):3152-3166. doi: 10.1109/TCE.2024.3363616

[28] Fischer J, Gumhold S. Fast and Accurate Parameter Conversion for Parametric Human Body Models. Proceedings of the ACM on Computer Graphics and Interactive Techniques. 2025; 8(4):1-21. doi: 10.1145/3747869

[29] Cai Z, Yin W, Zeng A, et al. Smpler-x: Scaling up expressive human pose and shape estimation. Advances in Neural Information Processing Systems. 2023; 36(1):11454-11468. doi: 10.52202/075280-0506

[30] Wu X, Yi J, Shi Y, et al. Design of dynamic ski motion capture and human posture detection model based on spatio-temporal Transformer and wireless device tracking technology. PeerJ Computer Science. 2023; 9(1):e1618-e1633. doi: 10.7717/peerj-cs.1618

[31] Giljarhus K E T, Liland F F, Oggiano L. Virtual skeleton methodology for athlete posture modification in CFD simulations. Sports Engineering. 2023; 26(1):39-45. doi: 10.1007/s12283-023-00430-8

[32] Sandeepkumar S, Jagan K. Optimizing Parameter Efficiency in Machine Learning Models: A Focus on Reducing Memory Overhead with L-BFGS-Optimized Algorithms. J. Electrical Systems. 2024; 20(5s):298-314. doi: 10.52783/jes.1948

[33] Mannel F. A Globalization of L-BFGS and the Barzilai-Borwein Method for Nonconvex Unconstrained Optimization. Journal of Optimization Theory and Applications. 2025; 204(3):47-80. doi: 10.1007/s10957-024-02565-5

[34] Bhatti U A, Tang H, Wu G, et al. Deep learning with graph convolutional networks: An overview and latest applications in computational intelligence. International Journal of Intelligent Systems. 2023; 2023(1):8342104-8342131. doi: 10.1155/2023/8342104

[35] Zhou T, Shen Y, Chen K, et al. Hierarchical dual graph convolutional network for aspect-based sentiment analysis. Knowledge-Based Systems. 2023; 276(1):110740-110749. doi: 10.1016/j.knosys.2023.110740